Received: 9 May 2018 | Revised: 12 June 2018 | Accepted: 18 June 2018

DOI: 10.1002/ddr.21442



WILEY DDR

RESEARCH ARTICLE

# The compound 2-(naphthalene-2-thio)-5,8-dimethoxy-1,4-naphthoquinone induces apoptosis via reactive oxygen species-regulated mitogen-activated protein kinase, protein kinase B, and signal transducer and activator of transcription 3 signaling in human gastric cancer cells

Jia-Ru Wang[1] | Gui-Nan Shen[1] | Ying-Hua Luo[2] | Xian-Ji Piao[3] | Meng Shen[4] | Chang Liu[1] | Yue Wang[1] | Ling-Qi Meng[1] | Yi Zhang[1] | Hao Wang[1] | Jin-Qian Li[1] | Wan-Ting Xu[1] | Yang Liu[1] | Hu-Nan Sun[1] | Ying-Hao Han[1] | Mei-Hua Jin[1] | Long-Kui Cao[4] | Cheng-Hao Jin[1,4]

| Enabling Technologies | | Strategy, Management & Health Policy | |
|---|---|---|---|
| Hit, Lead & Candidate Discovery | Preclinical Research & Development | Clinical Research | Post-Market Research |

[1]Department of Biochemistry and Molecular Biology, College of Life Science & Technology, Heilongjiang Bayi Agricultural University, Daqing, China

[2]College of Animal Science & Veterinary Medicine, Heilongjiang Bayi Agricultural University, Daqing, China

[3]Department of Gynaecology and Obstetrics, The Fifth Affiliated Hospital of Harbin Medical University, Daqing, China

[4]College of Food Science & Technology, Heilongjiang Bayi Agricultural University, Daqing, China

**Correspondence**
Cheng-Hao Jin, College of Life Science and Technology, Heilongjiang Bayi Agricultural University, Daqing 163319, China.
Email: jinchenghao3727@qq.com
and
Long-Kui Cao, College of Food Science & Technology, Heilongjiang Bayi Agricultural University, Daqing 163319, China.
Email: caolongkui2013@163.com

**Funding information**
Heilongjiang Bayi Agricultural University, Grant/Award Number: XYB2012-14; Postdoctoral Scientific Research Foundation of Heilongjiang Province of China, Grant/Award Number: LBH-Q13132; Natural Science Foundation of Heilongjiang Province of China, Grant/Award Number: LC2015036

It is reported that 1,4-naphthoquinones and their derivatives have potent antitumor activity in various cancers, although their clinical application is limited by observed side effects. To improve the therapeutic efficacy of naphthoquinones in the treatment of cancer and to reduce side effects, we synthesized a novel naphthoquinone derivative, 2-(naphthalene-2-thio)-5,8-dimethoxy-1,4-naphthoquinone (NTDMNQ). In this study, we explored the effects of NTDMNQ on apoptosis in gastric cancer cells with a focus on reactive oxygen species (ROS) production. Our results demonstrated that NTDMNQ exhibited the cytotoxic effects on gastric cancer cells in a dose-dependent manner. NTDMNQ significantly induced mitochondrial-related apoptosis in AGS cells and increased the accumulation of ROS. However, pre-treatment with N-acetyl-L-cysteine (NAC), an ROS scavenger, inhibited the NTDMNQ-induced apoptosis. In addition, NTDMNQ increased the phosphorylation of p38 kinase and c-Jun N-terminal kinase (JNK) and decreased the phosphorylation of extracellular signal-regulated kinase (ERK), protein kinase B (Akt), and Signal Transducer and Activator of Transcription 3 (STAT3); these effects were blocked by mitogen-activated protein kinase (MAPK) inhibitor and NAC. Taken together, the present findings indicate that NTDMNQ-induced gastric cancer cell apoptosis via ROS-mediated regulation of the MAPK, Akt, and STAT3 signaling pathways. Therefore, NTDMNQ may be a potential treatment for gastric cancer as well as other tumor types.

Wang, Shen, and Luo contributed equally to this work.

  

**KEYWORDS**

2-(naphthalene-2-thio)-5,8-dimethoxy-1,4-naphthoquinone, apoptosis, gastric cancer cells, MAPK signaling pathway, reactive oxygen species

## 1 | INTRODUCTION

Gastric cancer (GC) is a common malignant tumor of the digestive system. According to a recent report, gastric cancer is the third leading cause of cancer death and the fifth most frequent cancer worldwide, particularly in Eastern Asia (Luo et al., 2016). Nearly two-thirds of new diagnoses take place in developing countries, with 42% occurring in China alone (Kong et al., 2016; Wu et al., 2017). At present, the most widely used treatments for gastric cancer include surgery, chemotherapy and radiotherapy (Zhang et al., 2016). Nevertheless, the overall prognosis is frequently poor; the relative 5-year survival rate for gastric cancer is lower than 30% (Zheng et al., 2014). A variety of chemotherapy drugs, including 5-fluorouracil (5-FU) and cisplatin have been used to treat gastric cancer; however, these drugs not only affect cancer cells but also normal cells (Van Cutsem et al., 2006; Wang et al., 2016). As a result, there is a need to identify novel, more effective and less toxic antitumor agents.

Apoptotic pathways are activated by various signals, including the MAPK, protein kinase B (Akt), and STAT3 signaling pathways (Kim et al., 2014; Sampson et al., 2015). The MAPK signaling pathways involving ERK, p38, and JNK play crucial roles in cell growth, development, differentiation, apoptosis, and cell growth arrest (Yu, Kim, Yu, & Kim, 2013) Many studies have suggested that Akt is activated by drugs, extracellular cytokines, pressure, and other factors, such as the phosphatidylinositol 3-kinase (PI3K) signaling pathway (Yang, Guo, Shao, & Gao, 2017). Activated Akt can induce tumor cell apoptosis via modulation of downstream signaling (Costa et al., 2015; Porta, Paglino, & Mosca, 2014). The STAT3 signaling pathway is constitutively activated in many cancer cells, such as gastric and breast cancer (Samsonov et al., 2013; Zhu, Wang, Guo, Liu, & Dong, 2016). Therefore, findings have shown that the MAPK, Akt, and STAT3 signaling pathways are viable therapeutic targets for cancer treatment.

ROS are generated during the metabolism of oxygen, which generates free radicals, including hydroxyl radicals ($OH^-$), superoxide anions ($O_2^-$), singlet oxygen, and hydrogen peroxide ($H_2O_2$) (Günes-Bayir et al., 2017; Luo et al., 2016). Previous studies have reported that the production of intracellular ROS is vital for redox balance, cell signaling, and cell growth. Under conditions of oxidative stress, increased ROS generation may overcome cellular antioxidant defenses and induce cancer cell apoptosis (Chen et al., 2017). Additionally, the accumulation of intracellular ROS also initiates the destruction of the mitochondrial membrane, indirectly bringing about the induction of apoptosis (Li, Zhang, & Wang, 2017). Therefore, the search for novel anticancer therapies may primarily concentrate on intercellular apoptosis-stimulating agents that are mediated by various pathways. One well-known molecular pathway that induces apoptosis is the production of ROS (Ren, Yin, Yu, & Xiao, 2017). At present, some anticancer drugs have been shown to increase the level of intracellular ROS, repressing cancer cell growth via modulation of the MAPK and Akt signaling pathways, the Bcl-2 associated X (Bax)/B-cell lymphoma-2 (Bcl-2) ratio, and cysteinyl aspartate-specific proteinase-3 (caspase-3) protein expression in clinical practice (Tsai et al., 2017; Yin et al., 2017). Together, these finding indicate that ROS could adjust cell growth and death via regulated apoptotic-related signaling pathways.

The compound 1,4-naphthoquinone is an organic compound that is reported to exhibit a variety of pharmacological properties involving anti-inflammatory, antimicrobial, antiviral and antitumor effects (Bhasin, Chettiar, Etter, Mok, & Li, 2013; Coelho-Cerqueira, Netz, Canto, Pinto, & Follmer, 2014; Hafeez et al., 2013). For example, 1,4-naphthoquinone fused Gold (i) N-heterocyclic carbene complexes could enhance cancer cell death and reduce tumor burden by perturb antioxidant homeostasis (McCall et al., 2017). Although 1,4-naphthoquinone derivatives may inhibit lung, breast and prostate cancer cell proliferation, they are not widely used as anticancer drugs because of their high toxicity and side effects (Bolton, Trush, Penning, Dryhurst, & Monks, 2000; O'Brien, 1991). Some studies have shown that naphthoquinone derivatives strong toxicity may be because of the hydroxyl in their structure. The Dihydroxy of C5 and C8 make quinones less electrophilic, but it seems to increase the efficiency of redox cycling and result in greater toxicity (Ollinger & Brunmark, 1991). Therefore, substitution of hydroxyl structure is an effective way to reduce the toxic effect. Indeed, our previous study showed that 1,4-naphthoquinone derivatives—2-butylsulfinyl-1,-4-naphthoquinone (BSNQ), and 2-octylsulfinyl-1,4-naphthoquinone (OSNQ) considerably decreased the cytotoxicity and increased antitumor activity in HCC cells (Liu, Shen et al., 2017).

In the present study, to better improve the antitumor activity and reduce toxicity of 1,4-naphthoquinone derivatives, we substituted the dihydroxy of C5 and C8 with methoxy, and then synthesized a novel naphthoquinone derivative named 2-(naphthalene-2-thio)-5,8-dimethoxy-1,4-naphthoquinone (NTDMNQ). Then, we investigated the cytotoxic effects, apoptotic effects, ROS generation effects, and underlying mechanisms of NTDMNQ in gastric cancer cells.

## 2 | MATERIALS AND METHODS

### 2.1 | Chemicals and reagents

The chemicals used in compound synthesis were purchased from the Sigma-Aldrich Chemical Company (St. Louis, MO). 5-FU (MedChem Express; Princeton, NJ) and NTDMNQ were dissolved in 100% dimethyl sulfoxide (DMSO, St. Louis, MO) to prepare a 20 mM stock solution, and stored at −20 °C. Other chemicals were analytical grade.

Roswell Park Memorial Institute (RPMI) 1,640, dulbecco's modified eagle's medium (DMEM), fetal bovine serum (FBS), penicillin, and streptomycin were purchased from Gibco (Waltham, MA). Annexin V apoptosis detection kit, 2′,7′-dichlorofluorescein diacetate (DCFH-DA) and NAC were obtained from the Beyotime Institute Biotechnology (Shanghai, China). ECL was obtained from Thermo Fisher Scientific (Waltham, MA). All antibodies were purchased from Santa Cruz Biotechnology Inc. (Dallas, TX).

## 2.2 | Synthesis of naphthazarin

$AlCl_3$ (142 g) and NaCl (28.3 g) were melted at 150–155 °C, and a mixture of 1,4-dimethoxybenzene (0.12 mol) and maleic anhydride (0.24 mol) was added to the melted mixture. The temperature was sustained at 170–175 °C for 1–2 min and the dark red melt was allowed to cool. Next, the distilled water (1,400 ml) and 98% HCl (100 ml) were added to the melt mixture and continuous mixed for 12 hr to generate naphthazarin (Chang et al., 2017).

## 2.3 | Synthesis of 1,4,5,8-tetramethoxynaphthalene

The mixture of naphthazarin (19.0 g), tetrahydrofuran ($C_4H_8O$, 200 ml), $Na_2S_2O_4$ (10.6 g), distilled water (200 ml), and tetrabutylammonium bromide ($C_{16}H_{36}BrN$, 2.0 g) were mixed for 1 hr. Then, a solution of $C_2H_6O_4S$ (25 ml), NaOH (40 ml), and $Na_2S_2O_4$ (10.6 g) were added to the mixture stirred for 22 hr at room temperature. The 1,4,5,8-tetramethoxynaphthalene was then recovered by filtration and recrystallized from petroleum ether (b.p. 90–120 °C) (Huot & Brassard, 2011; Xu, Guo, Xu, & Li, 2006).

## 2.4 | Synthesis of 5,8-dimethoxy-1,4-naphthoquinone

A solution of cerium ammonium nitrate (CAN, 54 g) in water was added dropwise to a solution of 1,4,5,8-tetramethoxynaphthalene (40.3 mol) in $CH_3CN$ (450 ml) and $CHCl_3$ (150 ml). The resulting mixture was then stirred at room temperature for 1 hr. The organic layer was separated, dried over sodium sulfate, and concentrated in vacuo. The residue was recrystallized from MeOH to give the title compound 5,8-dimethoxy-1,4-naphthoquinone (DMNQ; Shen et al., 2009; Sun et al., 2016).

## 2.5 | Synthesis of 2-(naphthalene-2-thio)-5,8-dimethoxy-1,4-naphthoquinone

The 1-naphthalenethiol (1.65 mmol) was added to a solution of DMNQ (1.38 mmol) and MeOH (30 ml). The mixture was then stirred at room temperaturefor 4 hr. A solution of sodium dichromate ($Na_2Cr_2O_7{\cdot}2H_2O$, 0.76 mmol) and 98% $H_2SO_4$ (0.23 mmol) was then added and stirred for 2 min. The acidic solution was extracted with dichloromethane ($CHCl_2$, 60 ml). The organic layer was washed with brine (40 ml), dried over anhydrous sodium sulfate, filtered, and then concentrated under reduced pressure. The residue was separated by chromatography (hexane: EtOAc = 1:4) to yield the title compound 2-(naphthalene-2-thio)-5,-8-dimethoxy-1,4-naphthoquinone (NTDMNQ).

Nuclear magnetic resonance (NMR) spectra were recorded on a JNM-AL 400 (400 MHz). Chemical shifts (d) are given in ppm downfield from tetramethylsilane (TMS) as the internal standard. MS spectra were collected with an AB SCIEX API 2000 LC/MS/MS (Applied Biosystems, Inc., Carlsbad, CA) and LCMS-IT-TOF (Shimadzu Scientific Inc., Beijing, China).

## 2.6 | Cell culture

The nine GC cells and two normal cells were purchased from American Type Culture Collection (ATCC; Rockville, MD). Because the liver is the important target organ for drug toxicity testing, and human lung fibroblasts (IMR-90) are extracted from embryonic cells, their primary properties has not transformed, which can directly reflect the toxicity effects in the toxicity study, we chosen the QSG-7701 and IMR-90 as controls.

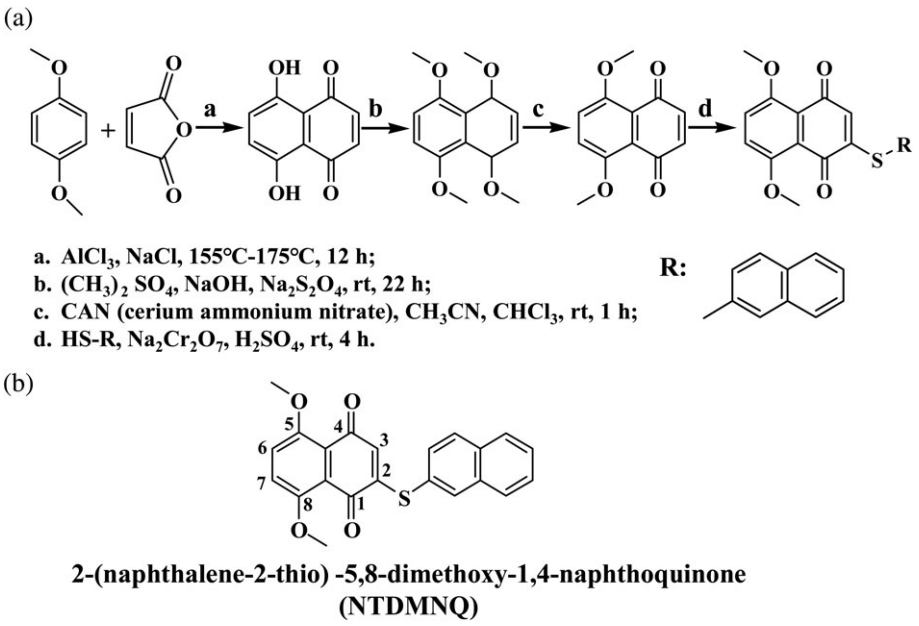


**FIGURE 1** The synthetic process and chemical structure identification of NTDMNQ

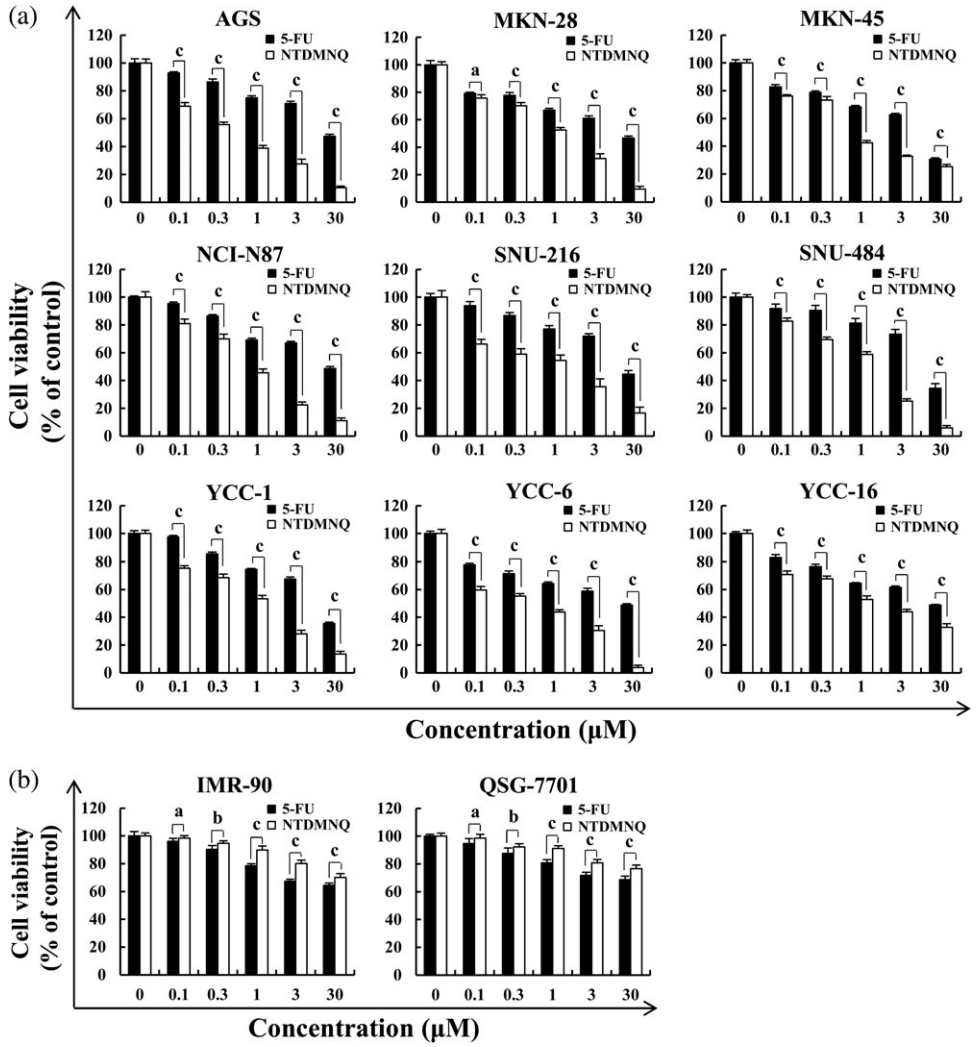


**FIGURE 2** Effects of NTDMNQ on cell viability in human gastric cancer cells. Nine human gastric cancer cell lines (AGS, MKN-28, MKN-45, NCI-N87, SNU-216, SNU-484, SNU-668, YCC-1, YCC-6, and YCC-16) and two normal cells (IMR-90 and QSG-7701) were treated with different concentrations (0.1, 0.3, 1.0, 3.0 and 30 μmol/L) of 5-FU or NTDMNQ for 24 hr. Error bars indicate means ± SD of three independent experiments ($^{a}p < 0.05$, $^{b}p < 0.01$, $^{c}p < 0.001$ indicate significant differences)

AGS, MKN-28, MKN-45, SNU-216, SNU-484, IMR-90, and QSG-7701 cells were maintained in RPMI 1640 medium. And NCI-N87, YCC-1, YCC-6, YCC-16 cells were grown in DMEM medium. Medium was supplemented with 10% FBS, 100 U/ml penicillin, and 100 μg/ml streptomycin. All cells were cultured in humidified atmosphere of 5% $CO_2$ at 37 °C, and cells were maintained at 80% confluence level.

## 2.7 | Cell viability assay

Cell viability was determined using the MTT assay. Gastric cancer cells (AGS, MKN-28, MKN-45, NCI-N87, SNU-216, SNU-484, YCC-1, YCC-6, and YCC-16) and normal human embryo lung IMR-90 cells and liver QSG-7701 cells were collected during the logarithmic phase of growth. All cells were seeded in 96-well plates at $1 \times 10^4$ cells/well, then treated with various doses (0.1, 0.3, 1.0, 3.0, and 30 μmol/L) of 5-FU and NTDMNQ for 24 hr. Adding the MTT solution (20 μl; 5 mg/ml) and cultured for 2 hr at 37 °C. Formazan crystals were lysed in 100 μl of DMSO, and cells were shocked for 10 min. Absorbance was then measured at a wavelength of 490 nm with an automatic micro-plate reader (BioTek Instruments Inc., Winooski, VT). Cell viability was expressed as the percentage change in absorbance compared to control values.

## 2.8 | Cell apoptosis analysis

Cell apoptosis was detected by the Annexin V apoptosis detection kit and flow cytometry. AGS cells were seeded in 6-well plates ($1 \times 10^5$ cells/well), and treated with 1 μmol/L 5-FU and NTDMNQ at 3, 6, 12, and 24 hr. Following treatment, the cells were collected and

**TABLE 1** $IC_{50}$ value of 5-FU and NTDMNQ in gastric cancer

| Cell name | 5-FU (μM) | NTDMNQ (μM) |
|---|---|---|
| AGS | 25.07 ± 3.02 | 0.42 ± 0.06 |
| MKN-28 | 17.96 ± 3.39 | 1.26 ± 0.05 |
| MKN-45 | 13.75 ± 1.84 | 0.82 ± 0.08 |
| SNU-216 | 27.89 ± 4.47 | 0.89 ± 0.13 |
| SNU-484 | 24.67 ± 3.49 | 1.44 ± 0.18 |
| NCI-N87 | 19.29 ± 2.62 | 1.53 ± 0.19 |
| YCC-1 | 17.81 ± 1.67 | 1.30 ± 0.15 |
| YCC-6 | 26.17 ± 3.29 | 0.80 ± 0.11 |
| YCC-16 | 27.59 ± 9.91 | 1.58 ± 0.69 |

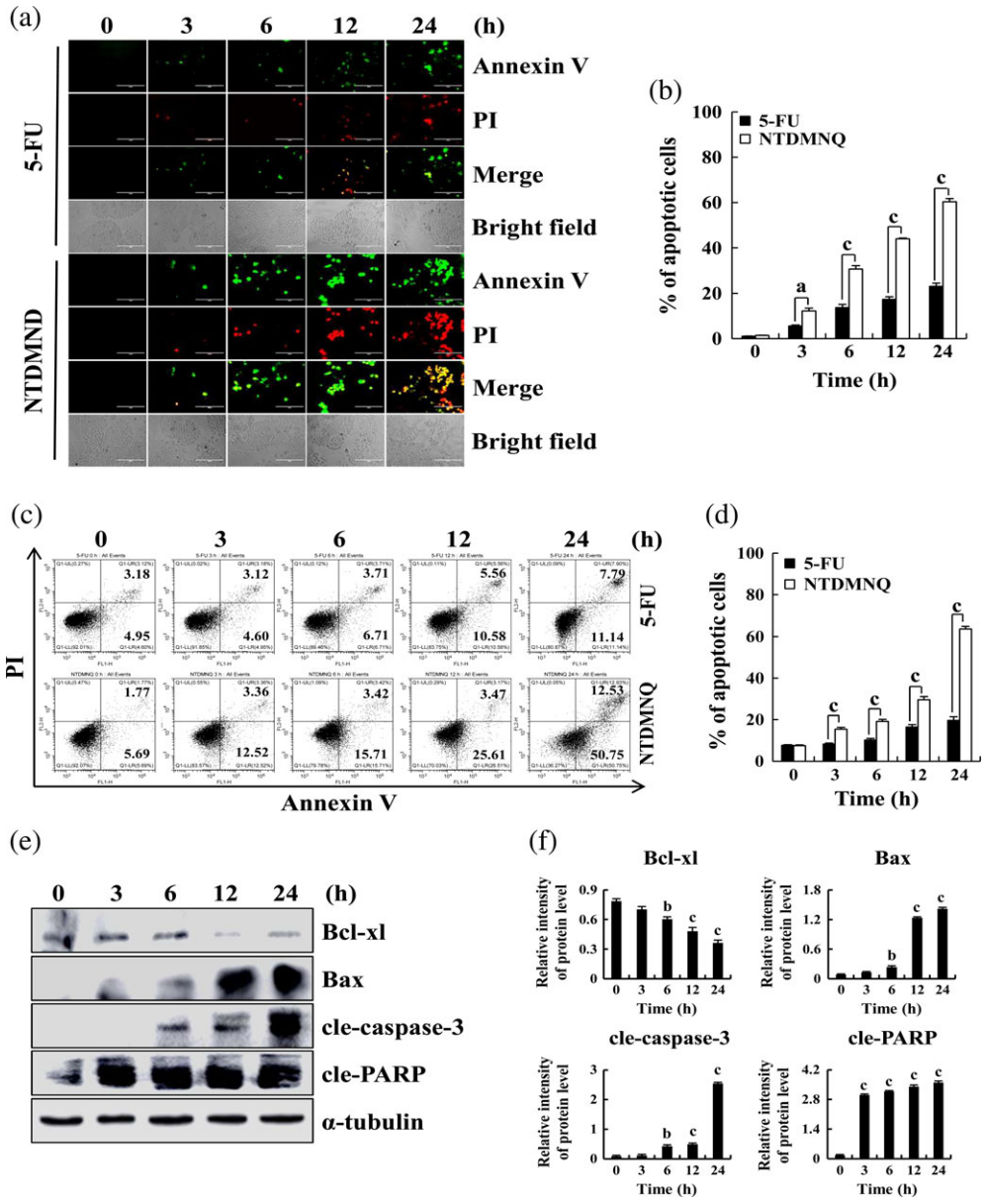


**FIGURE 3** Induction of apoptosis caused by NTDMNQ in AGS cells. (a) AGS cells were treated with 1 μmol/L of NTDMNQ and 5-FU for different time periods (3, 6, 12, and 24 hr), and stained with Annexin V-FITC/PI solution. The morphology and fluorescence intensity were observed under a fluorescence microscope (magnification: ×200). (b) Quantification of fluorescent intensity. (c) AGS cells were treated with the 1 μmol/L NTDMNQ and 5-FU for 3, 6, 12, and 24 hr, and stained with Annexin V-FITC/PI solution and analyzed by flow cytometer. (d) Quantification of the percentage of apoptotic cells. (e) Apoptosis-related proteins Bcl-xl, Bax, cleaved-PARP, and cleaved-caspase-3 expression levels were measured by western blotting. (f ) Quantification of the band density was analyzed by imageJ software. Error bars indicate means ± *SD* of three independent experiments ($^{a}p < 0.05$, $^{b}p < 0.01$, $^{c}p < 0.001$ indicate significant differences)

washed once in phosphate-buffered saline (PBS). Cells were resuspended in 195 μl Annexin V binding buffer, dual staining was performed with 3 μl Annexin V-FITC and 2 μl PI, and incubated for 20 min at the room temperature (RT) in the dark. Apoptotic cells were analyzed using the EVOS FL Auto Cell Imaging System (Thermo Fisher Scientific, Inc.) and flow cytometer (Beckman Coulter, Inc., Brea, CA).

## 2.9 | Western blotting analysis

Cells were extracted in lysis buffer, and then centrifuged for 30 min at 4 °C and 12,000 × g. The supernatants of 30 μg were electrophoresed on 8%–12% SDS-PAGE gels and then transferred onto nitrocellulose membranes. Membranes were blocked for 1 hr with 5% skim milk at RT, and then incubated overnight with primary antibodies against mouse monoclonal α-tubulin, Bax, Bcl-xl, Poly (ADP-ribose) polymerase-1 (PARP-1), cleaved caspase-3, p-ERK, p-JNK, JNK, p-p38, p-STAT3 (Tyr 705), and STAT3. Rabbit polyclonal ERK2, p38α/β, Akt, p-Akt at 4 °C (all from Santa Cruz Biotechnology, Inc., Dallas, TX). The membranes were washed in TBST, and incubated with Goat Anti-Rabbit IgG and Goat Anti-Mouse IgG secondary antibodies at rt for 2 hr. Following incubations, Pierce ECL was added, bands were detected using an Amersham Imager 600 (GE, Fairfield, CT) and evaluated using ImageJ software. Relative protein expression in treated cells was compared to the control group. The endogenous control was α-tubulin.

### 2.10 | Measurement of ROS levels

The accumulation of intracellular ROS was determined by using DCFH-DA staining, and many studies have shown that DCFH-DA staining is one of the most widely used techniques for directly measuring the redox state of cells (Afri, Frimer, & Cohen, 2004; Eruslanov & Kusmartsev, 2010). AGS cells were treated with NTDMNQ (1 μmol/L) for 3, 6, 12, and 24 hr, followed by centrifuged for 5 min at 6,000 × g. Cells were washed once in PBS, and staining with 10 μmol/L DCFH-DA for an additional 30 min at 37 °C in darkness, then analyzed by flow cytometer.

### 2.11 | Statistical analysis

Statistical analysis was performed using SPSS 19.0 software, and results are represented as means ± *SD* and analysis of variance (one-way ANOVA). The value of $p < .05$ was considered statistically significant.

## 3 | RESULTS

### 3.1 | Identification of the compound's structure

To synthesize 1,4-naphthoquinone derivatives with improved anticancer activity, we performed a series of steps to modify its chemical structure (Figure 1a). The residue was separated by chromatography (hexane: EtOAc = 1:4) to isolate the compound NTDMNQ (Figure 1b). By performing NMR at a wavelength of 400 MHz, we analyzed the H and C spectra in the deuterated chloroform solvent and identified the following structures:

NTDMNQ: $^{1}$H NMR ($CDCl_3$, 400 MHz) δ 8.09 (s, 1H), 7.91 (m, 2H), 7.85 (d, J = 6.0 Hz, 1H), 7.58 (m, 2H), 7.50 (d, J = 6.8 Hz, 1H), 7.32 (d, J = 7.2 Hz, 1H), 7.20 (d, J = 7.2 Hz, 1H), 5.97 (s, 1H), 3.99 (s, 3H), 3.91 (s, 3H); $^{13}$C NMR ($CDCl_3$, 150 MHz) δ 182.00 (C-1), 181.75 (C-4), 154.37 (C-5), 153.37 (C-8), 153.7 (C-2), 134.76 (C-9′), 131.26 (C-1′), 130.02 (C-10′), 128.83 (C′-2), 127.96 (C′-8), 127.90 (C-5′), 127.7 (C-3), 121.27 (C-7), 120.96 (C-6), 120.66 (C-10), 119.60 (C-9), 56.98 ($OCH_3$), 56.89 ($OCH_3$), 127.68 (C′-4), 126.96 (C′-3), 121.27 (C′-7), 121.08 (C′-6); MS: m/z 399.31 $(M + Na)^+$

These results confirm the successful synthesis of NTDMNQ.

### 3.2 | NTDMNQ inhibited the viability of gastric cancer cells

As shown in Figure 2a, NTDMNQ significantly inhibited the growth of nine different types of gastric cancer cells in a dose-dependent manner; the $IC_{50}$ values of 5-FU and NTDMNQ for each cell line show in Table 1. In addition, there were no obvious cytotoxic effects of NTDMNQ compared with 5-FU-treated group on IMR-90 and QSG-7701 cells (Figure 2b). Because the AGS cells showed higher sensitivity to NTDMNQ compared with other gastric cancer cells, we chose the AGS cells for further study.

### 3.3 | NTDMNQ-induced apoptosis in AGS cells

Compared to the control group, treatment with 5-FU and NTDMNQ for 24 hr caused morphological changes in the cells, specifically, a change from an inerratic rhombus to a spherical particle (Figure 3a,b). Additionally, the fluorescent intensity of the AGS cells was gradually enhanced in a time-dependent manner. Compared with 5-FU-treated cells, the

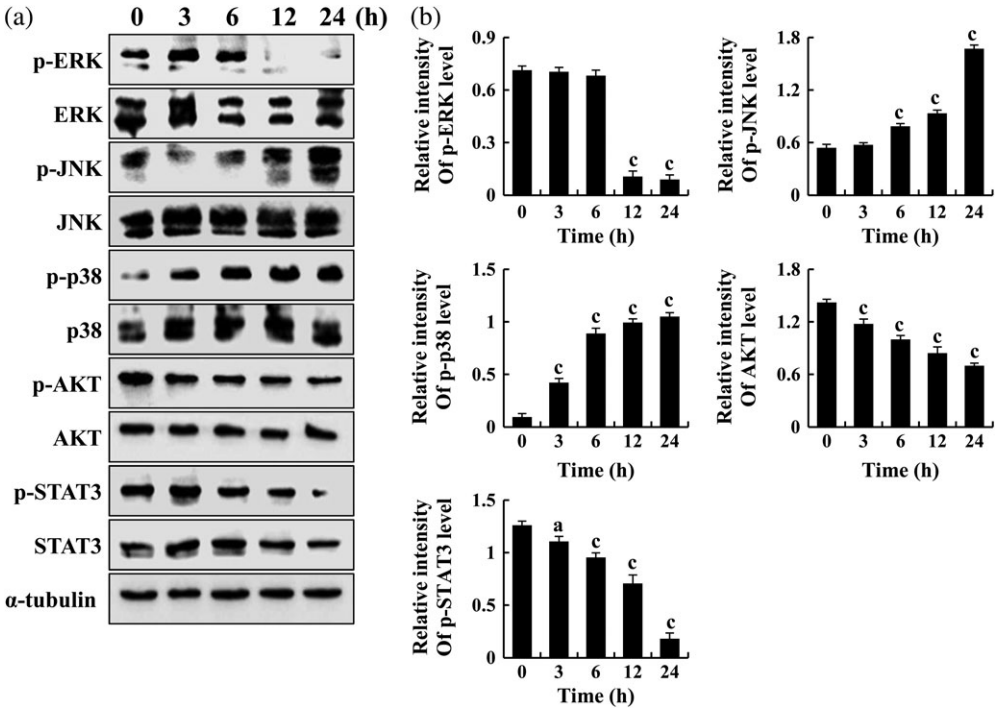


**FIGURE 4** Effects of NTDMNQ on MAPK, Akt, and STAT3 signaling pathways in AGS cells. (a) The expression levels of p-ERK, p-JNK, p-p38, p-Akt, and p-STAT3 were measured by western blotting, α-tubulin was used as an internal control. (b) Quantification of the p-ERK, p-JNK, p-p38, p-Akt, and p-STAT3 were analyzed by imageJ software. Error bars indicate means ± *SD* of three independent experiments ($^{a}p < 0.05$, $^{b}p < 0.01$, $^{c}p < 0.001$ indicate significant differences)

fluorescent intensity was markedly increased in the NTDMNQ-treated group. As shown in Figure 3c,d, there was a small percentage (7.46%) of apoptotic cells at 0 hr, and treatment with NTDMNQ for 24 hr dramatically increased apoptotic cells to 63.68%. This was significantly higher than the 5-FU-treated group. In addition, NTDMNQ significantly increased the protein expression levels of Bax, cleaved-caspase-3, and cleaved-PARP, while decreasing the protein expression levels of Bcl-xl (Figure 3e,f). Taken together, these indicated that NTDMNQ-induced apoptosis in AGS cells via regulating the mitochondrial apoptotic pathways.

### 3.4 | NTDMNQ regulated the MAPK, Akt, and STAT3 signaling pathways

As shown in Figure 4, NTDMNQ significantly decreased the levels of p-ERK, p-Akt, and p-STAT3, and increased the levels of p-JNK and p-p38 in a time-dependent manner. Thus, NTDMNQ induced apoptosis via the regulation of the MAPK, Akt, and STAT3 signaling pathways in AGS cells.

### 3.5 | NTDMNQ induced apoptosis by accelerating ROS generation in AGS cells

As shown in Figure 5a,b, NTDMNQ significantly increased intercellular ROS accumulation in a time-dependent manner. However, pretreatment with NAC apparently decreased NTDMNQ-induced apoptosis (Figure 5c,d). In addition, NAC markedly increased the expression levels of p-ERK, p-Akt, and p-STAT3, and decreased the expression levels of p-JNK, p-p38, and cleaved-caspase-3 (Figure 5e,f). These findings demonstrate that ROS generation is a key regulator of NTDMNQ-induced apoptosis. In addition, the

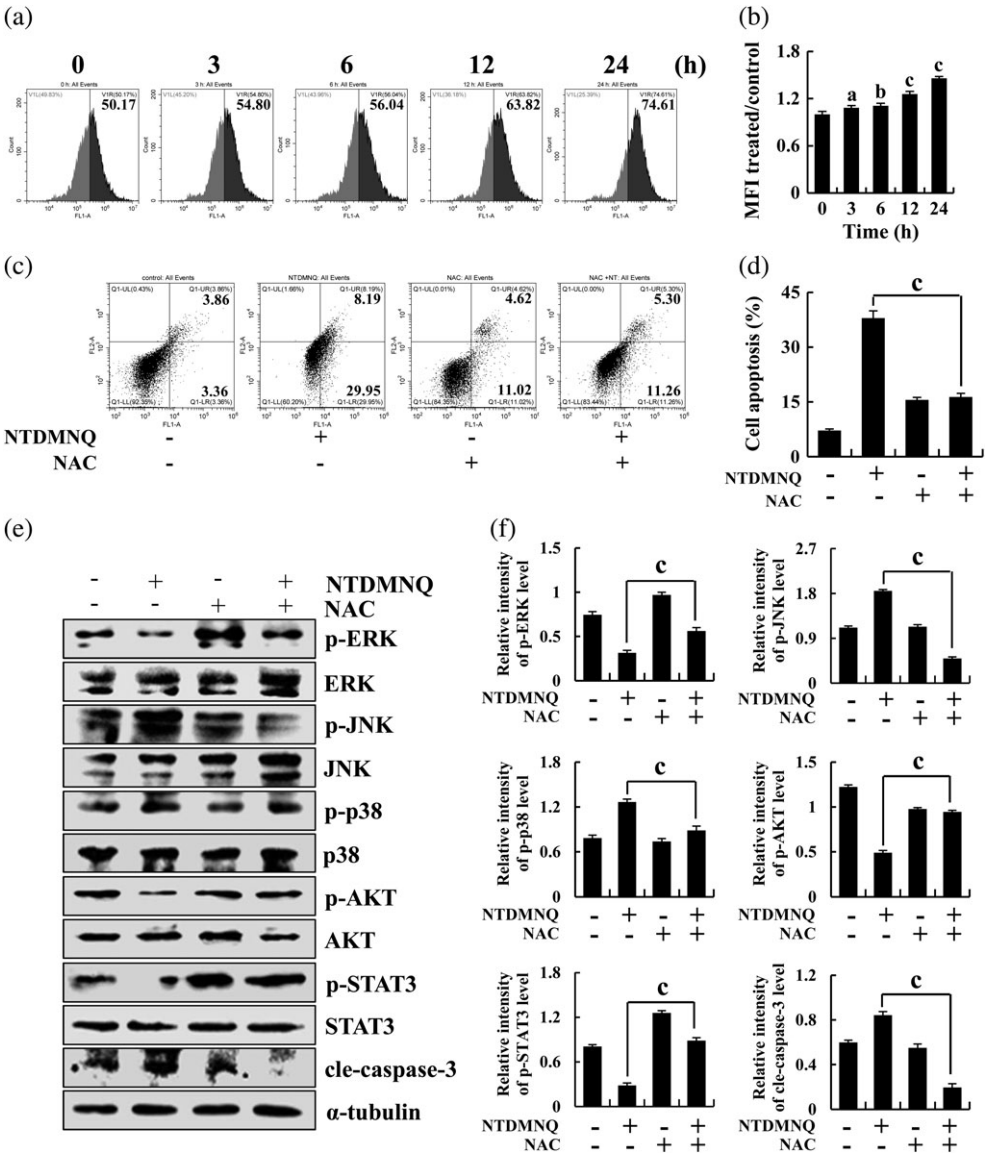


**FIGURE 5** The effects of NTDMNQ-induced ROS generation and apoptosis in AGS cells. (a,b) AGS cells were treated with NTDMNQ (1 μmol/L) and intracellular ROS generation measured by flow cytometer. (c,d) Inhibition of NTDMNQ-induced apoptosis. AGS cells were pretreated with NAC (5 μmol/L) for 30 min, then treated with NTDMNQ (1 μmol/L) for 24 hr. apoptosis was determined by flow cytometer. (e,f) p-ERK, p-JNK, p-p38, p-Akt, p-STAT3, cleaved-caspase-3, and cleaved-PARP protein expression levels were determined by western blotting. Error bars indicate means ± *SD* of three independent experiments ($^{a}p < 0.05$, $^{b}p < 0.01$, $^{c}p < 0.001$ indicate significant differences)

FR180204 (ERK inhibitor), SP600125 (JNK inhibitor), and SB203580 (p38 inhibitor) were used to further investigate the role of MAPK and STAT3 signaling pathways in cells apoptosis driven by NTDMNQ. The protein expression level of p-STAT3 was enhanced by ERK inhibitor, and this effect was inhibited by JNK inhibitor or p38 inhibitor (Figure 6a–f). These results suggested that MAPK was involved in mediating the STAT3 signaling pathway and induced AGS cells apoptosis.

## 4 | DISCUSSION

Naphthoquinone derivatives have been reported to have various pharmacological activities, such as anti-inflammatory, antiviral, and especially anticancer properties (Lee et al., 2011). In addition, several naphthoquinone derivatives promote the apoptosis of cancer cells via an ROS-dependent mechanism (Ong, Yong, Lim, & Ho, 2015). However, studies with naphthoquinone derivatives

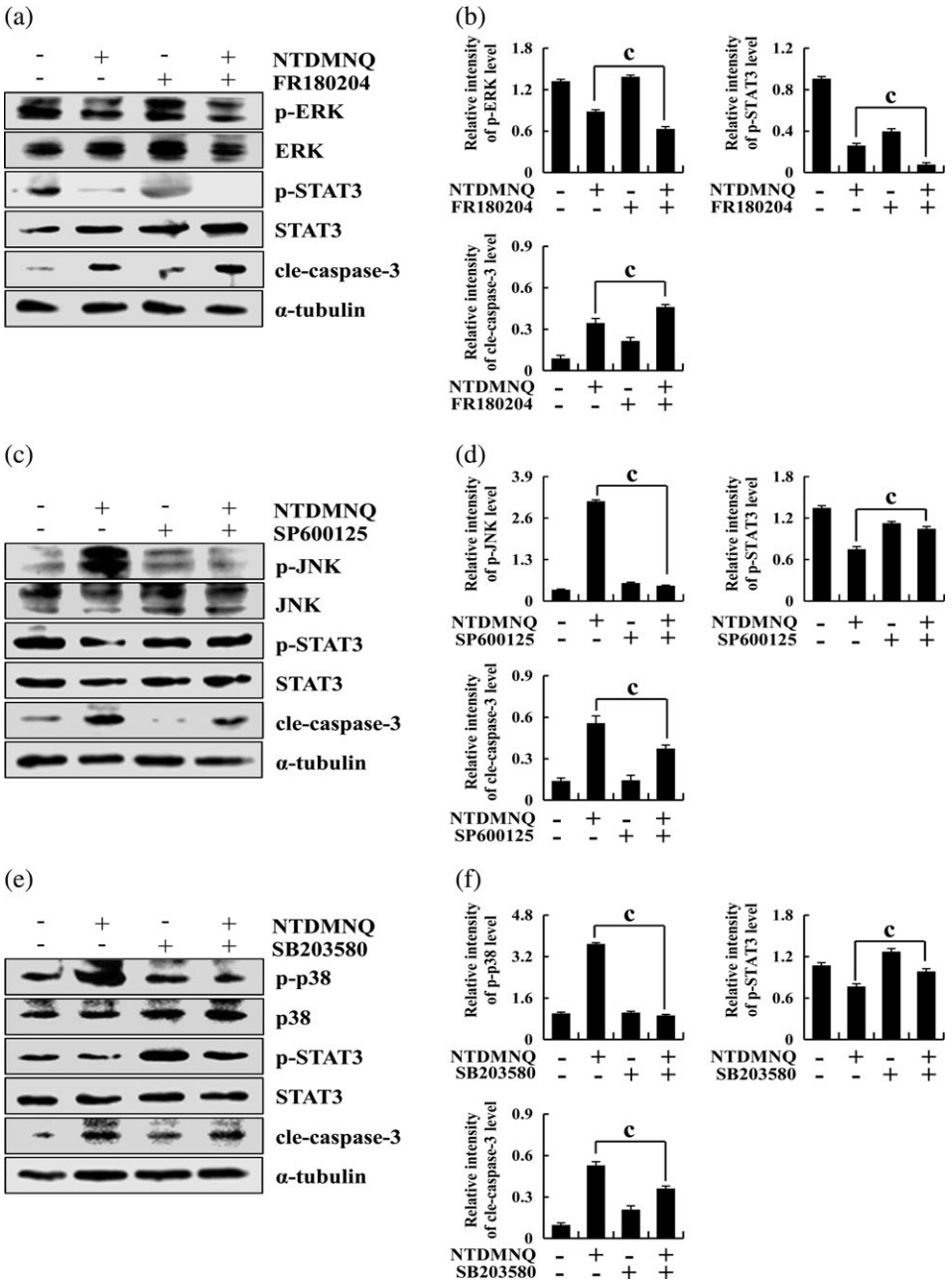


**FIGURE 6** The effects of NTDMNQ on MAPK and STAT3 signaling pathways in AGS cells. (a) AGS cells were pretreatment with 12.1 μmol/L of FR180204 for 30 min, and then treated with NTDMNQ for 24 hr, the expression levels of p-ERK, p-STAT3, and cleaved-caspase-3 were determined by western blotting. (b) Quantification of the p-ERK, p-STAT3, and cleaved-caspase-3 were analyzed by imageJ software. (c) AGS cells were pretreatment with 12.1 μmol/L of SP600125 for 30 min, and then treated with NTDMNQ for 24 hr, the expression levels of p-JNK, p-STAT3, and cleaved-caspase-3 were determined by western blotting. (d) Quantification of the p-JNK, p-STAT3, and cleaved-caspase-3 were analyzed by imageJ software. (e) AGS cells were pretreatment with 12.1 μmol/L of SB203580 for 30 min, and then treated with NTDMNQ for 24 hr, the expression levels of p-p38, p-STAT3, and cleaved-caspase-3 were determined by western blotting. (f) Quantification of the p-p38, p-STAT3, and cleaved-caspase-3 were analyzed by imageJ software. Error bars indicate means ± *SD* of three independent experiments ($^{a}p < 0.05$, $^{b}p < 0.01$, $^{c}p < 0.001$ indicate significant differences)

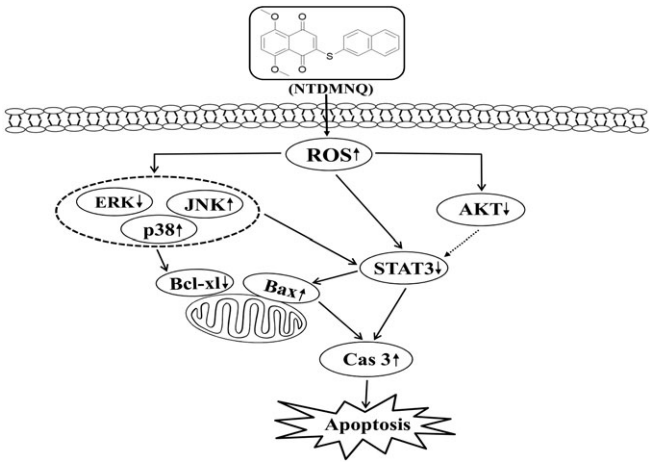


**FIGURE 7** Schematic illustration of the underlying mechanism of NTDMNQ effects on signaling pathways and the induction of apoptosis in gastric cancer cells. The mechanism of NTDMNQ anticancer activity as related to the MAPK, Akt, and STAT3 signal pathways

indicated that these compounds exhibit significant toxicity, possibly due to the hydroxyl group in their structure (Ollinger & Brunmark, 1991). To reduce their toxicity and improve the antitumor activity of compound, we substituted the dihydroxy groups at C5 and C8 with methoxy groups and then synthesized a novel naphthoquinone derivative called NTDMNQ (Figure 1). Our results showed that NTDMNQ-treated gastric cancer cells exhibited considerably higher rates of apoptosis than control treated cells (Figure 3b,c). These results were equivalent to the MTT assay results, which showed that NTDMNQ suppressed the proliferation of nine kinds of gastric cancer cells in a dose-dependent manner (Figure 2). Therefore, we hypothesized that the loss of viability in gastric cells treated with NTDMNQ is likely because of the induction of apoptosis.

Apoptosis as a cell defense mechanism that plays an important role in inhibiting tumor development (Zhu et al., 2012). Apoptosis has two primary pathways: The extrinsic and the intrinsic mitochondrial pathways, and among them, the Bcl-2 family members are known to mediate the apoptotic process (Yu, Kim, Yu, & Kim, 2013). It was reported that Ramentaceone, a naphthoquinone derivative, induced apoptosis in breast cancer cells by increasing the expression levels of the pro-apoptotic proteins Bax, cleaved-caspase-3, and cleaved-PARP, and decreasing the expression level of the anti-apoptotic protein Bcl-xl via inhibition of the PI3K/Akt signaling pathway (Kawiak & Lojkowska, 2016). Similarly, our results suggested that NTDMNQ induced apoptosis via decreasing the protein expression level of Bcl-xl and increasing the expression levels of pro-apoptotic protein Bax, cleaved-caspase-3, and cleaved-PARP (Figure 3e,f ). In addition, it has been reported that 5-hydroxy-1,4-naphthalenedione (juglone) which is 1,4-naphthoquinione derivative may interact with the mitochondrial electron transfer chain (ETC) in mitochondria. The intracellular free radical production by quinones is thought to be a consequence of $O_2$ reduction by semiquinone intermediates. The semiquinone is formed via one-electron reduction of the corresponding quinone catalyzed by NADPH-cytochrome $P_{450}$ reductase. The structures of juglone are similar to the compound which we synthesized (Ollinger & Brunmark, 1991; Sidlauskas, Sidlauskiene, Li, & Liobikas, 2017; Zhang, Hirsch, Mohsen, & Samuni, 1994). On the basis of the above, we speculate that NTDMNQ could interfere with the mitochondrial electron transfer chain and induced apoptosis via regulating the mitochondrial apoptotic pathways.

Recent studies have shown that ROS can induce apoptosis in various cell systems (Ma et al., 2014). The ROS plays a central role in cellular survival and function, although cell death was caused by excessive generation of ROS-induced oxidative stress (Chien et al., 2014). Some studies show that the highly redox active naphthoquinones undergo one-electron reduction when the organs with a sufficient blood supply and in an aerobic conditions, and generate free-radical intermediates, resulting in the accumulation of ROS (Qiu et al., 2018; Wellington, 2015). Our study indicated that NTDMNQ induced apoptosis through increasing intracellular ROS levels (Figure 5a,b). NAC is an antioxidant with ROS scavenging that have a potentially benefits effect for the treatment of diseases (Aldini et al., 2018). Because of the NAC that have well-described antioxidant and radical scavenging activity, it has also been used as an antioxidant in several in many studies (Dodd, Dean, Copolov, Malhi, & Berk, 2008). Such as, NAC could inhibit the quinalizarin-induced ROS generation in lung cancer A549 cells and blocked cryptotanshinone-induced apoptosis in gastric cancer cells (Liu et al., 2017; Meng et al., 2018). In this study, to determine the relationship of NTDMNQ-induced apoptosis and ROS, the NAC was used to pretreat the AGS cells. And the result shows that NAC significantly inhibited NTDMNQ-induced apoptosis by decreasing ROS levels (Figure 5c,d). These findings clearly demonstrate our hypothesis that NTDMNQ-induced apoptosis in AGS cells via up-regulating the generation of ROS. In addition, ROS have been demonstrated to induce apoptosis in malignant tumor cells by activating the caspase, MAPK, PI3K/Akt, and STAT3 signaling pathways (Miao, Yu, Ren, & Yang, 2017; Zhong et al., 2016). MAPK is a family of serine/threonine kinases. It was reported that the activation of p38 and JNK induces apoptosis via the phosphorylation of various pro-apoptotic downstream effectors, while the ERK pathway is primarily associated with cell survival (Lohberger et al., 2015; Shin et al., 2012). Studies have shown that naphthoquinone derivatives activate the ERK, JNK and p38 signaling pathways by stimulating ROS generation (Ong et al., 2015). The activation of STAT3 and Akt may be a key mechanism in the treatment of a variety of cancers (Wu et al., 2013). In addition, Akt may regulate apoptosis via modulation of Bcl-2 family members (Zhang et al., 2012). The STAT3 signaling pathway is also a key anti-apoptotic pathway in cancer cells because it is associated with cell proliferation, immune evasion, and apoptotic arrest (Liu et al., 2015; Wang, Tang, & Zhang, 2017). These effects are most likely mediated through ROS-induced activation of the STAT3 pathway (Miao, Yu, Ren, & Yang, 2017). Therefore, we investigated the cellular signaling pathways involved in NTDMNQ-induced apoptosis. Our results showed that p38 and JNK phosphorylation was markedly increased after NTDMNQ-treated, and ERK, Akt, and STAT3 phosphorylation was significantly decreased (Figure 4). Furthermore, NAC inhibited MAPK, Akt, and STAT3 activation, which indicates that NTDMNQ-induced apoptosis in AGS cells by the ROS-mediated MAPK, Akt, and STAT3 signaling pathways (Figure 5e,f ). Additionally, to determine whether STAT3 was regulated by NTDMNQ-induced MAPK activation, the MAPK inhibitor (including FR180204, SP600125, and

SB203580) were used to investigate the relation between MAPK and STAT3. These data suggested that the reactivation of the MAPK inhibitor via NTDMNQ-inhibited the STAT3 signaling pathway, demonstrating that STAT3 was regulated through the MAPK signaling pathway (Figure 6).

## 5 | CONCLUSIONS

In summary, we synthesized a novel naphthoquinone derivative, 2-(naphthalene-2-thio)-5,8-dimethoxy-1,4-naphthoquinone (NTDMNQ), and the anticancer molecular mechanisms of NTDMNQ were investigated. NTDMNQ induce apoptosis in human GC cells through ROS-mediated MAPK/Akt/STAT3 signaling pathways (Figure 7). Based on our observations, NTDMNQ may be a candidate for the development and exploitation of antigastric cancer drugs.

### ACKNOWLEDGMENTS

This work was funded by the Natural Science Foundation of Heilongjiang Province of China (LC2015036), the Postdoctoral Scientific Research Foundation of Heilongjiang Province of China (LBH-Q13132), the Research Project of Heilongjiang Bayi Agricultural University (XYB2012-14), and the Scientific Research Foundation of Heilongjiang Provincial Education Department of China (1252HQ007).

### CONFLICT OF INTEREST

The authors declare they have no conflict of interest.

### AUTHORS' CONTRIBUTIONS

C.-H. J and D.-J. Z.: conceived and designed the experiments; J.-R. W., G.-N. S., and Y.-H. L.: wrote the article and participated in the experiment; X.-J. P., C. L., and L.-Q. M.: assessed the cytotoxic effects; Y. W. and Y. Z.: performed the apoptotic analysis; H. W., W.-T. X., J.-Q. L., and Y. L.: performed western blotting analysis; H.-N. S., Y.-H. H., and M.-H. J. performed the signaling analysis; All authors read and approved the final version of the manuscript.

### ORCID

*Cheng-Hao Jin* http://orcid.org/0000-0003-4431-2623

### REFERENCES

Afri, M., Frimer, A. A., & Cohen, Y. (2004). Active oxygen chemistry within the liposomal bilayer. Part IV: Locating 2′,7′-dichlorofluorescein (DCF), 2′,7′-dichlorodihydrofluorescein (DCFH) and 2′,7′-dichlorodihydrofluorescein diacetate (DCFH-DA) in the lipid bilayer. *Chemistry and Physics of Lipids*, *131*(1), 123–133. https://doi.org/10.1016/j.chemphyslip.2004.04.006

Aldini, G., Altomare, A., Baron, G., Vistoli, G., Carini, M., Borsani, L., & Sergio, F. (2018). N-acetylcysteine as an antioxidant and disulphide breaking agent: The reasons why. *Free Radical Research*, *9*, 1–12. https://doi.org/10.1080/10715762.2018.1468564

Bhasin, D., Chettiar, S. N., Etter, J. P., Mok, M., & Li, P. K. (2013). Anticancer activity and SAR studies of substituted 1,4-naphthoquinones. *Bioorganic & Medicinal Chemistry*, *21*(15), 4662–4669. https://doi.org/10.1016/j.bmc.2013.05.017

Bolton, J. L., Trush, M. A., Penning, T. M., Dryhurst, G., & Monks, T. J. (2000). Role of quinones in toxicology. *Chemical Research in Toxicology*, *13*(3), 135–160.

Chang, G., Zhou, Y., Zhu, R. Z., Liu, Z. H., Cao, Y. B., & Cao, R. B. (2017). Method for synthesizing 5,8-dihydroxy-1,4-naphthoquinone with molten salt. China, Patent NO. 201710669130.8.

Chen, X., Dai, X., Zou, P., Chen, W., Rajamanickam, V., Feng, C., … Liang, G. (2017). Curcuminoid EF24 enhances the anti-tumour activity of Akt inhibitor MK-2206 through ROS-mediated endoplasmic reticulum stress and mitochondrial dysfunction in gastric cancer. *British Journal of Pharmacology*, *174*(10), 1131–1146. https://doi.org/10.1111/bph.13765

Chien, C. C., Wu, M. S., Shen, S. C., Ko, C. H., Chen, C. H., Yang, L. L., … Chen, Y. C. (2014). Activation of JNK contributes to evodiamine-induced apoptosis and G2/M arrest in human colorectal carcinoma cells: A structure-activity study of evodiamine. *PLoS One*, *9*(6), e99729. https://doi.org/10.1371/journal.pone.0099729

Coelho-Cerqueira, E., Netz, P. A., Canto, V. P. D., Pinto, A. C., & Follmer, C. (2014). Beyond topoisomerase inhibition: Antitumor 1,4-naphthoquinones as potential inhibitors of human monoamine oxidase. *Chemical Biology & Drug Design*, *83*(4), 401–410. https://doi.org/10.1111/cbdd.12255

Costa, C., Pereira, S., Lima, L., Peixoto, A., Fernandes, E., Neves, D., … Santos, L. L. (2015). Abnormal protein glycosylation and activated PI3K/Akt/mTOR pathway: Role in bladder cancer prognosis and targeted therapeutics. *PLoS One*, *10*(11), e0141253. https://doi.org/10.1371/journal.pone.0141253

Dodd, S., Dean, O., Copolov, D. L., Malhi, G. S., & Berk, M. (2008). N-acetylcysteine for antioxidant therapy: Pharmacology and clinical utility. *Expert Opinion on Biological Therapy*, *8*(12), 1955–1962. https://doi.org/10.1517/14728220802517901

Eruslanov, E., & Kusmartsev, S. (2010). Identification of ROS using oxidized DCFDA and flow-cytometry. *Methods in Molecular Biology*, *594*, 57–72. https://doi.org/10.1007/978-1-60761-411-1_4

Günes-Bayir, A., Kiziltan, H. S., Kocyigit, A., Güler, E. M., Karataş, E., & Toprak, A. (2017). Effects of natural phenolic compound carvacrol on the human gastric adenocarcinoma (AGS) cells in vitro. *Anti-Cancer Drugs*, *28*(5), 522–530. https://doi.org/10.1097/CAD.0000000000000491

Hafeez, B. B., Zhong, W., Fischer, J. W., Mustafa, A., Shi, X., Meske, L., … Verma, A. K. (2013). Plumbagin, a medicinal plant (Plumbago zeylanica)-derived 1,4-naphthoquinone, inhibits growth and metastasis of human prostate cancer PC-3M-luciferase cells in an orthotopic xenograft mouse model. *Molecular Oncology*, *7*(3), 428–439. https://doi.org/10.1016/j.molonc.2012.12.001

Huot, R., & Brassard, P. (2011). Friedel–crafts condensations with maleic anhydrides III. The synthesis of polyhydroxylated naphthoquinones. *Canadian Journal of Chemistry*, *52*(5), 838–842.

Kawiak, A., & Lojkowska, E. (2016). Ramentaceone, a Naphthoquinone Derived from Drosera sp., Induces Apoptosis by Suppressing PI3K/Akt Signaling in Breast Cancer Cells. *PLoS One*, *11*(2), e0147718. https://doi.org/10.1371/journal.pone.0147718.

Kim, M. C., Lee, H. J., Lim, B., Ha, K. T., Kim, S. Y., So, I., & Kim, B. J. (2014). Quercetin induces apoptosis by inhibiting MAPKs and TRPM7 channels in AGS cells. *International Journal of Molecular Medicine*, *33*(6), 1657–1663. https://doi.org/10.3892/ijmm.2014.1704

Kong, G. M., Tao, W. H., Diao, Y. L., Fang, P. H., Wang, J. J., Bo, P., & Qian, F. (2016). Melittin induces human gastric cancer cell apoptosis via activation of mitochondrial pathway. *World Journal of Gastroenterology*, *22*(11), 3186–3195. https://doi.org/10.3748/wjg.v22.i11.3186

Lee, J. J., Zhang, W. Y., Yi, H., Kim, Y., Kim, I. S., Shen, G. N., … Myung, C. S. (2011). Anti-proliferative actions of 2-decylamino-5,8-dimethoxy-1,4-naphthoquinone in vascular smooth muscle cells. *Biochemical and Biophysical Research Communications*, *411*(1), 213–218. https://doi.org/10.1016/j.bbrc.2011.06.145

Li, H., Zhang, X., & Wang, W. (2017). Anticancer activity of 5, 7--dimethoxyflavone against liver cancer cell line HEPG2 involves apoptosis, ROS generation and cell cycle arrest. *African Journal of Traditional, Complementary, and Alternative Medicines*, *14*(4), 213–220. https://doi.org/10.21010/ajtcam.v14i4.24

Liu, C., Shen, G. N., Luo, Y. H., Piao, X. J., Jiang, X. Y., Meng, L. Q., … Jin, C. H. (2017). Novel 1,4-naphthoquinone derivatives induce

apoptosis via ROS-mediated p38/MAPK, Akt and STAT3 signaling in human hepatoma Hep3B cells. *International Journal of Biochemistry and Cell Biology*, *96*, 9–19. https://doi.org/10.1016/j.biocel.2018.01.004

Liu, C., Sun, H. N., Luo, Y. H., Piao, X. J., Wu, D. D., Meng, L. Q., … Jin, C. H. (2017). Cryptotanshinone induces ROS-mediated apoptosis in human gastric cancer cells. *Oncotarget*, *8*(70), 115398–115412. https://doi.org/10.18632/oncotarget.23267

Liu, Y. F., Lu, Y. M., Qu, G. Q., Liu, Y., Chen, W. X., Liao, X. H., & Kong, W. M. (2015). Ponicidin induces apoptosis via JAK2 and STAT3 signaling pathways in gastric carcinoma. *International Journal of Molecular Sciences*, *16*(1), 1576–1589. https://doi.org/10.3390/ijms16011576

Lohberger, B., Leithner, A., Stuendl, N., Kaltenegger, H., Kullich, W., & Steineckerfrohnwieser, B. (2015). Diacerein retards cell growth of chondrosarcoma cells at the G2/M cell cycle checkpoint via cyclin B1/CDK1 and CDK2 downregulation. *BMC Cancer*, *15*, 891–901. https://doi.org/10.1186/s12885-015-1915-4

Luo, D., Ni, Q., Ji, A., Gu, W., Wu, J., & Jiang, C. (2016). Dehydroabietic acid derivative QC4 induces gastric cancer cell death via Oncosis and apoptosis. *BioMed Research International*, *2016*(3), 1–10. https://doi.org/10.1155/2016/2581061

Luo, D., Xu, Z., Hu, X., Zhang, F., Bian, H., Li, N., … Gu, J. (2016). URI prevents potassium dichromate-induced oxidative stress and cell death in gastric cancer cells. *American Journal of Translational Research*, *8*(12), 5399–5409.

Ma, W. D., Zou, Y. P., Wang, P., Yao, X. H., Sun, Y., Duan, M. H., … Yu, B. (2014). Chimaphilin induces apoptosis in human breast cancer MCF-7 cells through a ROS-mediated mitochondrial pathway. *Food and Chemical Toxicology*, *70*, 1–8. https://doi.org/10.1016/j.fct.2014.04.014

McCall, R., Miles, M., Lascuna, P., Burney, B., Patel, Z., Sidoran, K. J., … Arambula, J. F. (2017). Dual targeting of the cancer antioxidant network with 1,4-naphthoquinone fused gold(i) N-heterocyclic carbene complexes. *Chemical Science*, *8*(9), 5918–5929. https://doi.org/10.1039/c7sc02153d

Meng, L. Q., Liu, C., Luo, Y. H., Piao, X. J., Wang, Y., Zhang, Y., … Jin, C. H. (2018). Quinalizarin exerts an anti-tumour effect on lung cancer A549 cells by modulating the Akt, MAPK, STAT3 and p53 signalling pathways. *Molecular Medicine Reports*, *17*(2), 2626–2634. https://doi.org/10.3892/mmr.2017.8110

Miao, Z., Yu, F., Ren, Y., & Yang, J. (2017). D,l-Sulforaphane induces ROS-dependent apoptosis in human Gliomablastoma cells by inactivating STAT3 signaling pathway. *International Journal of Molecular Sciences*, *18*(1), 72–85. https://doi.org/10.3390/ijms18010072

O'Brien, P. J. (1991). Molecular mechanisms of quinone cytotoxicity. *Chemico-Biological Interactions*, *80*(1), 1–41.

Ollinger, K., & Brunmark, A. (1991). Effect of hydroxy substituent position on 1,4-naphthoquinone toxicity to rat hepatocytes. *The Journal of Biological Chemistry*, *266*(32), 21496–21503.

Ong, J. Y., Yong, P. V., Lim, Y. M., & Ho, A. S. (2015). 2-Methoxy-1,4-naphthoquinone (MNQ) induces apoptosis of A549 lung adenocarcinoma cells via oxidation-triggered JNK and p38 MAPK signaling pathways. *Life Sciences*, *135*, 158–164. https://doi.org/10.1016/j.lfs.2015.03.019

Porta, C., Paglino, C., & Mosca, A. (2014). Targeting PI3K/Akt/mTOR signaling in cancer. *Frontiers in Oncology*, *4*(4), 64–74. https://doi.org/10.3389/fonc.2014.00064

Qiu, H. Y., Wang, P. F., Lin, H. Y., Tang, C. Y., Zhu, H. L., & Yang, Y. H. (2018). Naphthoquinones: A continuing source for discovery of therapeutic antineoplastic agents. *Chemical Biology & Drug Design*, *91*(3), 681–690. https://doi.org/10.1111/cbdd.13141

Ren, H. P., Yin, X. Y., Yu, H. Y., & Xiao, H. F. (2017). Stevioside induced cytotoxicity in colon cancer cells via reactive oxygen species and mitogen-activated protein kinase signaling pathways-mediated apoptosis. *Oncology Letters*, *13*(4), 2337–2343. https://doi.org/10.3892/ol.2017.5744

Sampson, V. B., Vetter, N. S., Kamara, D. F., Collier, A. B., Gresh, R. C., & Kolb, E. A. (2015). Vorinostat enhances cytotoxicity of SN-38 and Temozolomide in Ewing sarcoma cells and activates STAT3/AKT/-MAPK pathways. *PLoS One*, *10*(11), e0142704. https://doi.org/10.1371/journal.pone.0142704

Samsonov, A., Zenser, N., Zhang, F., Zhang, H., Fetter, J., & Malkov, D. (2013). Tagging of genomic STAT3 and STAT1 with fluorescent proteins and insertion of a luciferase reporter in the cyclin D1 gene provides a modified A549 cell line to screen for selective STAT3 inhibitors. *PLoS One*, *8*(7), e68391. https://doi.org/10.1371/journal.pone.0068391

Shen, G. N., Choi, J. H., Gajulapati, K., Lee, J. H., Kim, Y. K., Rho, M. C., … Choi, Y. (2009). 2-Substitiuted Thio- and Amino-5,8-dimethoxy-1,4-naphthoquinones as a novel class of acyl-CoA: Cholestrol acyltransferase inhibitors. *Bulletin of the Korean Chemical Society*, *30*(5), 1088–1092.

Shin, D. Y., Kim, G. Y., Lee, J. H., Choi, B. T., Yoo, Y. H., & Choi, Y. H. (2012). Apoptosis induction of human prostate carcinoma DU145 cells by Diallyl disulfide via modulation of JNK and PI3K/AKT signaling pathways. *International Journal of Molecular Sciences*, *13*(11), 14158–14171. https://doi.org/10.3390/ijms131114158

Sidlauskas, K., Sidlauskiene, R., Li, N., & Liobikas, J. (2017). 5-Hydroxy-1,4-naphthalenedione exerts anticancer effects on glioma cells through interaction with the mitochondrial electron transport chain. *Neuroscience Letters*, *639*, 207–214. https://doi.org/10.1016/j.neulet.2017.01.007

Sun, H. N., Shen, G. N., Jin, Y. Z., Jin, Y., Han, Y. H., Feng, L., … Jin, C. H. (2016). 2-cyclohexylamino-5,8-dimethoxy-1,4-naphthoquinone inhibits LPS- induced BV2 microglial activation through MAPK/NF-kB signaling pathways. *Heliyon*, *2*(7), e00132. https://doi.org/10.1016/j.heliyon.2016.e00132

Tsai, M. H., Liu, J. F., Chiang, Y. C., Hu, S. C., Hsu, L. F., Lin, Y. C., … Lee, C. W. (2017). Artocarpin, an isoprenyl flavonoid, induces p53-dependent or independent apoptosis via ROS-mediated MAPKs and Akt activation in non-small cell lung cancer cells. *Oncotarget*, *8*(17), 28342–28358. https://doi.org/10.18632/oncotarget.16058

Van Cutsem, E., Moiseyenko, V. M., Tjulandin, S., Majlis, A., Constenla, M., Boni, C., & V325, Study. Group. (2006). Phase III study of docetaxel and cisplatin plus fluorouracil compared with cisplatin and fluorouracil as first-line therapy for advanced gastric cancer: A report of the V325 study group. *Journal of Clinical Oncology*, *24*(31), 4991–4997. https://doi.org/10.1200/JCO.2006.06.8429

Wang, D., Tang, S., & Zhang, Q. (2017). Maslinic acid suppresses the growth of human gastric cells by inducing apoptosis via inhibition of the interleukin-6 mediated Janus kinase/signal transducer and activator of transcription 3 signaling pathway. *Oncology Letters*, *13*(6), 4875–4881. https://doi.org/10.3892/ol.2017.6073

Wang, J., Xu, R., Li, J., Bai, Y., Liu, T., Jiao, S., … Shen, L. (2016). Randomized multicenter phase III study of a modified docetaxel and cisplatin plus fluorouracil regimen compared with cisplatin and fluorouracil as first-line therapy for advanced or locally recurrent gastric cancer. *Gastric Cancer*, *19*(1), 234–244. https://doi.org/10.1007/s10120-015-0457-4

Zhong, W. F., Wang, X. H., Pan, B., Li, F., Kuang, L., & Su, Z. X. (2016). Eupatilin induces human renal cancer cell apoptosis via ROS-mediated MAPK and PI3K/AKT signaling pathways. *Oncology Letters*, *12*(4), 2894–2899. https://doi.org/10.3892/ol.2016.4989

Wellington, K. W. (2015). Understanding cancer and the anticancer activities of naphthoquinones-a review. *RSC Advances*, *46*(20), 20309–20355. https://doi.org/10.1039/C4RA13547D

Wu, H., Liu, S., Gong, J., Liu, J., Zhang, Q., Leng, X., … Li, Y. (2017). VCPA, a novel synthetic derivative of α-tocopheryl succinate, sensitizes human gastric cancer to doxorubicin-induced apoptosis via ROS-dependent mitochondrial dysfunction. *Cancer Letters*, *393*, 22–32. https://doi.org/10.1016/j.canlet.2017.02.007

Wu, K., Chang, Q., Lu, Y., Qiu, P., Chen, B., Thakur, C., … Chen, F. (2013). Gefitinib resistance due to STAT3-mediated Akt activation in lung cancer cells. *Oncotarget*, *4*(12), 2430–2438. https://doi.org/10.18632/oncotarget.1431

Xu, D. F., Guo, X. J., Xu, Z. H., & Li, S. S. (2006). A novel Total synthesis of (±) Shikonin. *Chinese Chemical Letters*, *17*(7), 871–873.

Yang, Y., Guo, J. X., Shao, Z. Q., & Gao, J. P. (2017). Matrine inhibits bladder cancer cell growth and invasion in vitro through PI3K/AKT signaling pathway: An experimental study. *Asian Pacific Journal of Tropical Medicine*, *10*(5), 515–519. https://doi.org/10.1016/j.apjtm.2017.05.009

Yin, Z., Zhao, X., Yang, D., Cao, X., Yu, Y., Jiang, H., … Guo, Q. (2017). LFG-500, a newly synthesized flavonoid, induces apoptosis in human ovarian carcinoma SKOV3 cells with involvement of the reactive oxygen species-mitochondria pathway. *Experimental and Therapeutic Medicine*, *13*(6), 2819–2827. https://doi.org/10.3892/etm.2017.4343

Yu, S. M., Kim, S. J., Yu, S.-M., & Kim, S.-J. (2013). Thymoquinone-induced reactive oxygen species causes apoptosis of chondrocytes via PI3K/Akt and p38kinase pathway. *Experimental Biology and Medicine*, *238*(7), 811–820. https://doi.org/10.1177/1535370213492685

Zhang, D. M., Liu, J. S., Tang, M. K., Yiu, A., Cao, H. H., Jiang, L., … Ye, W. C. (2012). Bufotalin from Venenum Bufonis inhibits growth of multidrug resistant HepG2 cells through G2/M cell cycle arrest and apoptosis. *European Journal of Pharmacology*, *692*(1–3), 19–28. https://doi.org/10.1016/j.ejphar.2012.06.045

Zhang, R., Hirsch, O., Mohsen, M., & Samuni, A. (1994). Effects of nitroxide stable radicals on juglone cytotoxicity. *Archives of Biochemistry and Biophysics*, *1312*(2), 385–391.

Zhang, Y., Xu, W., Ni, P., Li, A., Zhou, J., & Xu, S. (2016). MiR-99a and MiR-491 regulate cisplatin resistance in human gastric cancer cells by targeting CAPNS1. *International Journal of Biological Sciences*, *12*(12), 1437–1447. https://doi.org/10.7150/ijbs.16529

Zheng, L., Wu, C., Xi, P., Zhu, M., Zhang, L., Chen, S., … Zheng, Y. (2014). The survival and the long-term trends of patients with gastric cancer in Shanghai, China. *BMC Cancer*, *14*(1), 300–311. https://doi.org/10.1186/1471-2407-14-300

Zhu, W. Q., Wang, J., Guo, X. F., Liu, Z., & Dong, W. G. (2016). Thymoquinone inhibits proliferation in gastric cancer via the STAT3 pathway in vivo and in vitro. *World Journal of Gastroenterology*, *22*(16), 4149–4159. https://doi.org/10.3748/wjg.v22.i16.4149

Zhu, Z., Sun, H., Ma, G., Wang, Z., Li, E., Liu, Y., & Liu, Y. (2012). Bufalin induces lung cancer cell apoptosis via the inhibition of PI3K/Akt pathway. *International Journal of Molecular Sciences*, *13*(2), 2025–2035. https://doi.org/10.3390/ijms13022025

**How to cite this article:** Wang J-R, Shen G-N, Luo Y-H, et al. The compound 2-(naphthalene-2-thio)-5,8-dimethoxy-1,4-naphthoquinone induces apoptosis via reactive oxygen species-regulated mitogen-activated protein kinase, protein kinase B, and signal transducer and activator of transcription 3 signaling in human gastric cancer cells. *Drug Dev Res*. 2018; 1–12. https://doi.org/10.1002/ddr.21442